OPTICAL PROPERTIES OF THE ANALBITE-HIGH SANIDINE SOLID SOLUTION SERIES

Julie K. Warner

Submitted to the department of Geological Sciences of
Virginia Polytechnic Institute and State University
in partial fulfillment of the
requirements for the degree of

BACHELOR OF SCIENCE IN HONORS
August 1984

ABSTRACT

OPTICAL PROPERTIES OF THE ANALBITE-HIGH SANIDINE SOLID SOLUTION SERIES

For homogeneous, high-temperature alkali feldspars, precise spindle stage measurements of the refractive indices n_a, n_b and n_c -- those for sodium light vibrating most nearly parallel to the $\underline{a}$, $\underline{b}$, and $\underline{c}$ crystallographic axes, respectively -- indicate that they vary linearly with mol % Or ($R^2 > 0.976$). The lines for n_b and n_c cross at ~ 72% Or (for $2t_1 \cong 0.56$). Thus 2Vx is 0° for that composition and varies sigmoidally (not linearly as previously assumed) from ~68° for analbite and ~ 52° for high sanidine. Concomitantly, the optic axial plane (OAP) changes from approximately perpendicular to (010) to parallel to (010). The n_a (or α) refractive index seems to have the best correlation with composition for high temperature alkali feldspars because it is the parameter least sensitive to chemical and structural variations. Corrections for these differences in minor substituents and structural state need to be employed before meaningful correlations are determined between all optical properties and composition.

ACKNOWLEDGEMENTS

I would like to thank Mr. ShuChun Su for the many hours of help and insight he contributed to this research. Without his inspiration I could not have completed this project. I appreciate the unlimited patience of Dr. Paul H. Ribbe and the additional support from Dr. F. Donald Bloss, Dr. J. Donald Rimstidt and Mr. Mark Miller. Also, I wish to acknowledge the staff of the drafting department of Marathon Oil Company, in particular Mr. Dan Oberly and Mr. Rich Adair, for their help of drafting the figures for this paper.

TABLE OF CONTENTS

Title: Optical Properties of the Analbite-High Sanidine Solid Solution Series

INTRODUCTION

Because of the petrologic importance of feldspars, there is much interest in the relationships among their compositions, their optical and other properties, and their structural states. The optic axial angle (2V) is known to be related to the degree of Al,Si order-disorder ("structural state") of the alkali feldspars, but until recently, the most efficient way to determine structural state has been to measure unit cell parameters by x-ray powder or single-crystal methods. Using the $\underline{b}$-$\underline{c}$ and $\alpha^* - \gamma^*$ plots or the determinative equations of Kroll and Ribbe (1983), it is now possible to calculate Al,Si distributions among the 2 (or 4) non-equivalent tetrahedral sites of any alkali feldspar, regardless of composition or symmetry.

Plotting the $\underline{b}$ and $\underline{c}$ cell edges against each other produces a quadrilateral (Figure 1) in which lines parallel to the upper and lower edges on the plot define alkali feldspars of equivalent structural state where structural state is defined as $[t_1o + t_1m]$ = total Al content of the T_1o and T_1m tetrahedral sites (Stewart and Ribbe, 1969). The upper edge is the low albite-low microcline limiting series which represents the highest degree of order of Al into the T_1o site ($t_1o = 1.0$; $t_1m = 0.0$). The lower edge is defined by the analbite-high sanidine series, which ideally is completely disordered with regard to the probability of finding Al in a particular T_1 site, i.e., $t_1o = t_1m = 0.25$. The right and left edges represent alkali feldspars of a constant composition (Na-rich and K-rich, respectively), where structural state varies from completely ordered (low albite and low microcline) to completely disordered (analbite and high sanidine).

Figure 1

The b-c plot, produced by plotting the b and c cell dimensions against each other. Contours represent degree of disorder and numbered points are compositions in % Or. (Modified from Kroll and Ribbe, 1983).

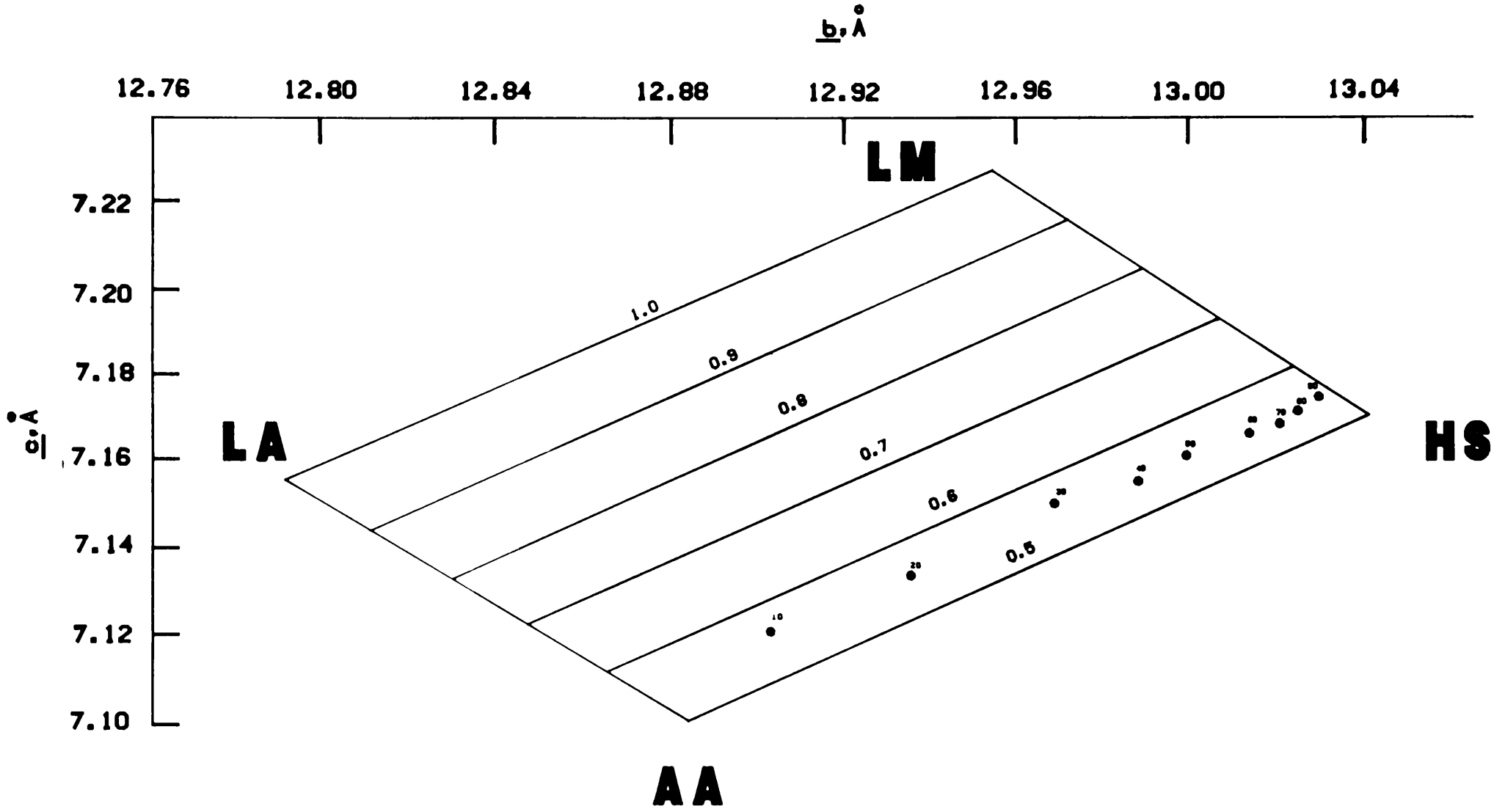
b, Å
12.76
12.80
12.84
12.88
12.92
12.96
13.00
13.04
LM
7.22
7.20
7.18
7.16
7.14
7.12
7.10
c, Å
LA
HS
AA
1.0
0.9
0.8
0.7
0.6
0.5

In an attempt to find a simpler method for determining structural state, Su et al. (1984) studied the low microcline-high sanidine series of K-rich feldspars. Following an idea advanced by Hewlett (1959), they designated the refractive index of light vibrating most nearly parallel to the a crystallographic axis as n_a, that most nearly parallel to b as n_b, and that most nearly parallel to c as n_c (instead of the conventional α, β, and γ). In this way, it is possible to compare the refractive indices for light vibrating along similar crystallographic directions for orientations of the optical indicatrix which vary with both structural state and compostition (Su et al., 1984). It is known that the optic axial plane (OAP) inverts from apporximately perpendicular to (010) in low microcline to parallel to (010) in high sanidine (see Figure 2). The authors plotted the refractive index curves assuming linearity and showed that the n_b and n_c lines must cross to accommodate this inversion. Therefore, $\gamma = n_b$ and $\beta = n_c$ for low microcline whereas $\gamma = n_c$ and $\beta = n_b$ for high sanidine. Figure 3 demonstrates this, and also shows that 2V values from the literature fit well to a sigmoidal curve which must pass through $2V = 0°$ at the point where n_b and n_c cross. This has made it possible to determine structural state for K-rich feldspars (>80 mol% orthoclase) with a simple measurement of 2Vx.

Using this and other existing data for 2Vx of alkali feldspars of differing compositions and structural states, the b-c plot was contoured preliminarily for optic axial angle by Stewart and Ribbe (1983). See Figure 4.

Various series of alkali feldspars with accurately determined optical, chemical, and structural state measurements are needed to more

Figure 2

Diagram showing optic orientation for low microcline and high sanidine. The optic axial plane (OAP) inverts from approximately perpendicular to (010) in low microcline to parallel to (010) in high sanidine. (Su et. al., 1984).

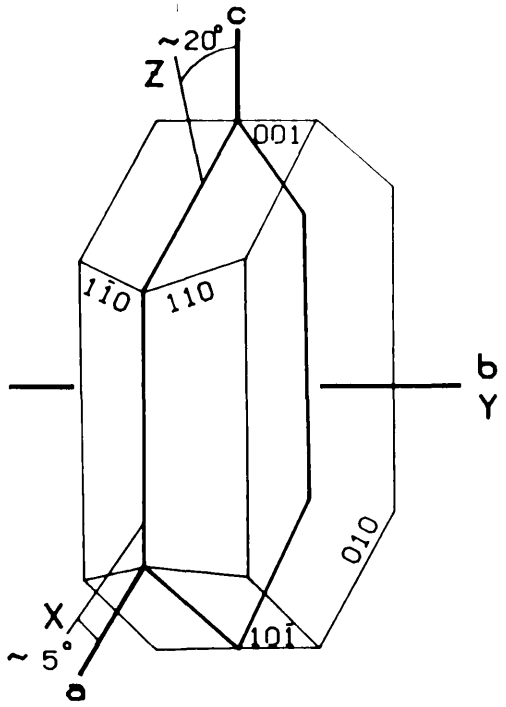

HIGH SANIDINE

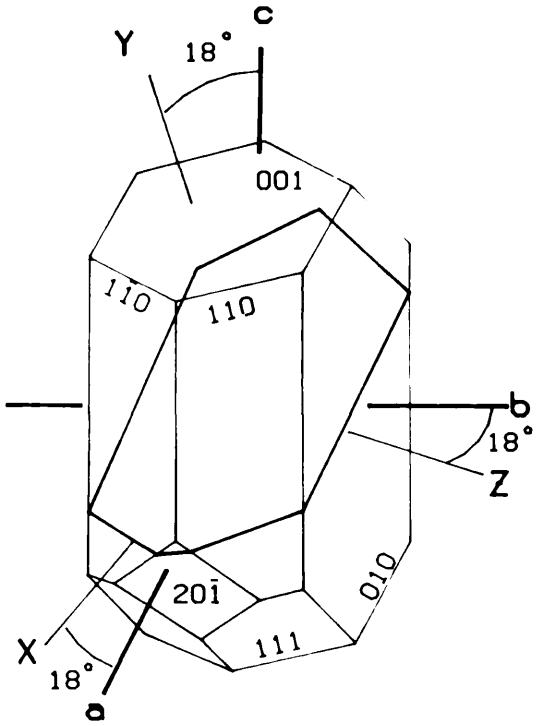

LOW MICROCLINE

Figure 3

Relationship between refractive index and structural state ($t_1o + t_1m$) for K-rich feldspars. The n_b and n_c lines cross at ~.67 and the resulting 2Vx curve is a sigmoidal function. (Su et. al., 1984).

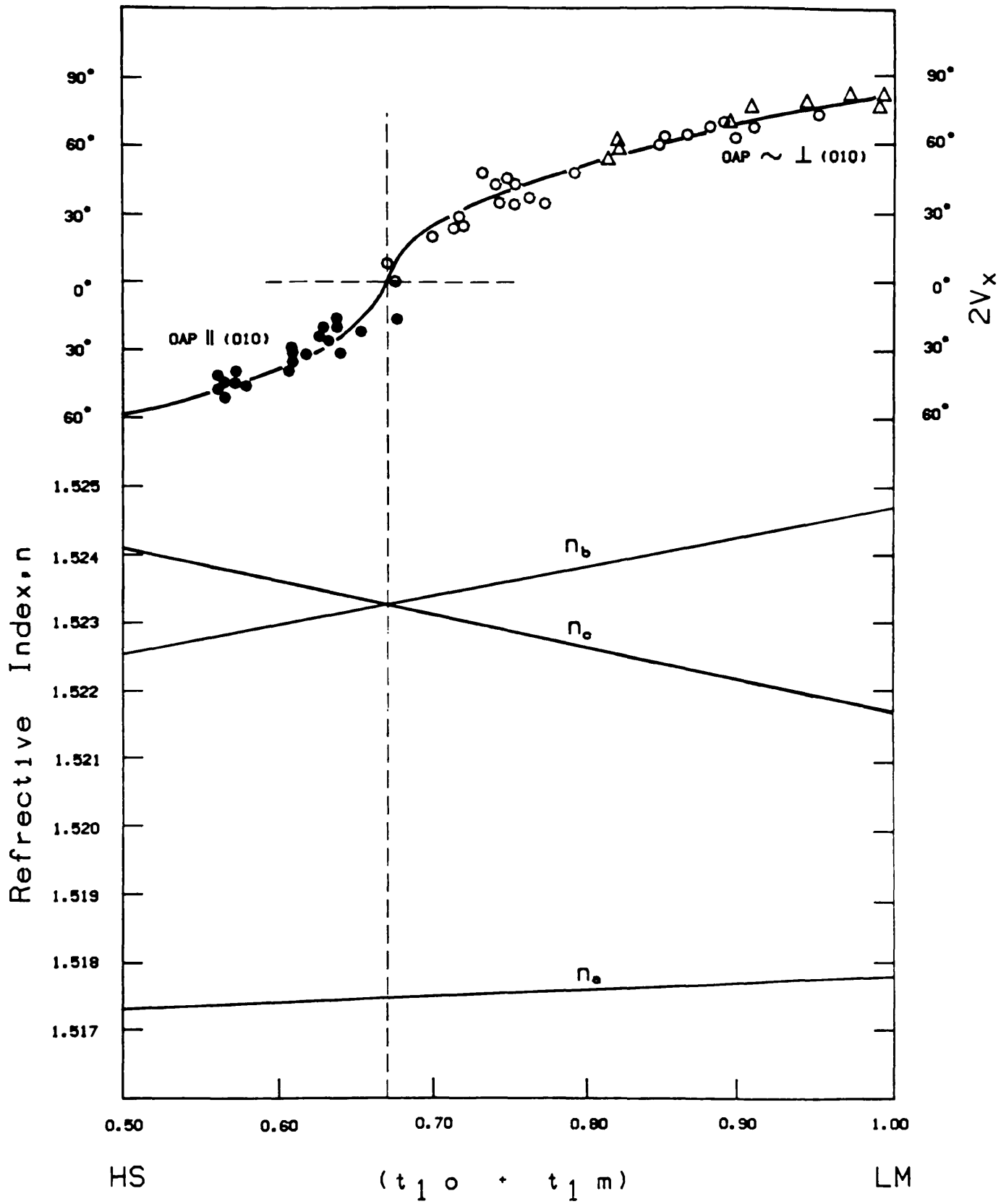

△ TRICLINIC OAP ~ ⊥ (010)

○ MONOCLINIC OAP ⊥ (010)

● MONOCLINIC OAP ∥ (010)

Figure 4

The b-c plot contoured for optic axial angle, 2V, Most of the data is centered around the K-rich series and uncertainty in the contours result. (Modified from Stewert and Ribbe, 1983).

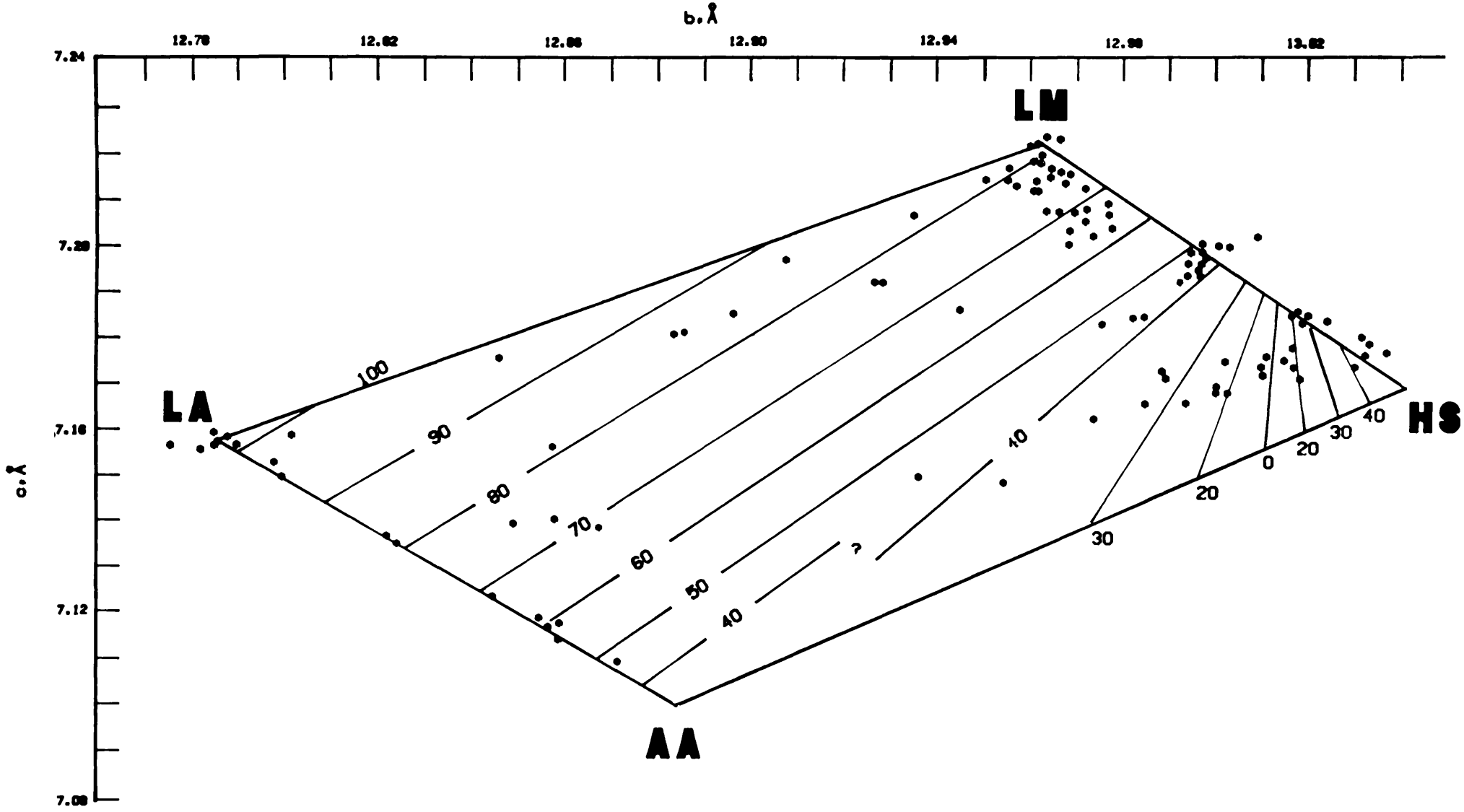
b, Å
12.78
12.82
12.86
12.90
12.94
12.98
13.02
7.24
7.20
7.16
7.12
7.08
c, Å
LM
LA
AA
HS
100
90
80
70
60
50
40
40
30
20
0
20
30
40

precisely locate the 2V contours on the b-c plot. Most of the data used to contour the b-c plot fall near the low microcline-high sanidine series; high quality data are almost entirely lacking for the other three series which define the boundaries of the b-c plot, namely the low albite-analbite, low albite-low microcline, and analbite-high sanidine series.

Recent developments in the spindle stage technique (Bloss, 1981) have make it possible to measure optic axial angle and refractive indices of a crystal to accuracies never routinely achieved before. And, using single-crystal x-ray techniques, it is possible to determine accurate cell dimensions on the same crystal without having to remount it. When optical and x-ray studies are completed, and orientation of the optical indicatrix relative to the crystallographic axes has been established, the crystal can be mounted in epoxy and polished so that microprobe analysis can be performed on that very grain for determination of its chemical composition. This permits accurate comparison of all properties characteristic of one particular grain; previously data was collected from a number of grains within a given sample in which properties vary slightly from grain to grain.

The purpose of this research is to precisely define relations between optical properties and composition and eventually structural state for one of the limiting series of the b-c plot -- the analbite-high sanidine series -- using these techniques. It is known that the orientation of the optic axial plane for analbite is approximately perpendicular to (010) and that of high sanidine is parallel to (010). See Figure 5. Therefore, like the K-rich feldspars, the n_b and n_c refractive index curves must cross and the 2Vx curve must

Figure 5

Diagrams showing optic orientations for analbite and high sanidine. Like the K-rich feldspars, the optic axial plane inverts from approximately perpendicular to (010) to parallel to (010). Therefore, the n_b and n_c lines must also cross.

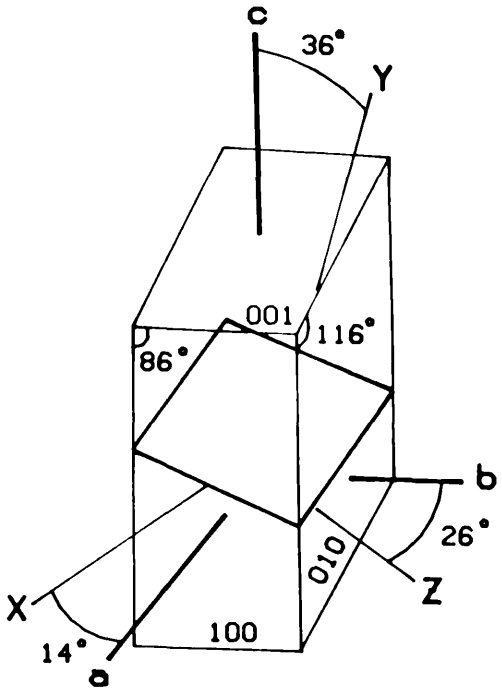

ANALBITE

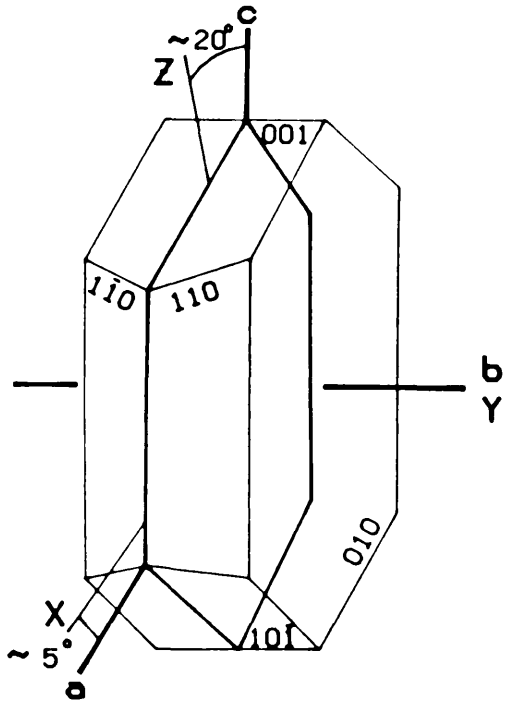

HIGH SANIDINE

pass through 0°. This work is aimed at determining the variation of refractive indices with composition and the nature of the resulting sigmiodal 2V curve. The minor substituents -- $[(Ca^{2+} + Ba^{2+} + Sr^{2+}) + Al^{3+}] \leftrightharpoons [(Na^{+} + K^{+}) + Si^{4+}]$, and $Fe^{3+} \leftrightharpoons Al^{3+}$ -- are of concern in this sort of investigation, but their effects on refractive indices (and 2V) had to be overlooked because of a limited data base and limited time.

EXPERIMENTAL PROCEDURES

Alkali feldspars used in this study were selected from samples that were relatively pure (low Ca, Ba, and Sr content) and of presumably high structural state (i.e., formed at high temperatures). The crystals used were optically homogenous and exhibited good (010) and (001) cleavages, which expedited the identification of the crystallographic axes in both direct and reciprocal space.

Three of the samples, although optically homogeneous later proved either to be submicroscopically twinned, exsolved, or both, as indicated by back-reflection x-ray photographs. These were not used in the study, although their optical data were plotted for comparison with others from true single crystals. It is thought that perhaps these crystals represent lower structural states than the others, because twinning and/or exsolution often accompanies inversion from monoclinic to triclinic structures, and this usually occurs at lower temperatures. Attempts to heat these crystals at 1000°C for 100 hours failed due to lack of precise temperature control and consequent melting of the outer surface of the grains.

Optical properties determined from so-called "composite crystals" will be an average of the optics of the phases or domains present, because they are smaller than the wavelength of light used (Hauser and Wenk, 1976). It would be interesting to unravel the effects of each domain on the optics of the composite, but this was not possible within the limits of the present study.

Data for samples closer to the high albite and high sanidine end members were chosen from the literature to reduce the amount of extrapolation. See Table 1 for data on alkali feldspars in this study.

Optical Methods

The crystals (100 to 200 microns in size) were mounted with fingernail polish to a 1 cm long glass fiber. This was affixed with wax to a goniometer head, which has two adjustable eucentric arcs perpendicular to each other that allow the grain to be moved precisely (to within a tenth of a degree) to a desired orientation. The goniometer head was mounted on a Supper spindle stage or on an x-ray camera, both of which have an additional axis of rotation nearly parallel to the glass fiber.

Initially crystals were mounted with the a cell edge (the intersection of the (010) and (001) cleavage faces) parallel to the rotation axis of the goniometer head. In this orientation the crystal is ready for optical work but also can later be transferred to an x-ray camera to establish the location of the crystallographic axes and to obtain the photographs used for unit cell determination.

Determination of optic axial angle, 2V

With the goniometer head mounted on the Supper spindle stage, extinction positions were determined on a polarizing microscope (equipped with a photometer) at 10° increments of the spindle's 360° rotation axis. This was done at each of three wavelengths that

Table 1

Summary of samples used in this study. Two samples were from the literature and three were "composite" crystals which were used only for comparison with other data points.

SAMPLE	COMPOSITION (mol % Or)	REFERENCE
HIGH ALBITE	0.0	Tuttle and Bowen (1950)
3112	34.6	Carmichael (1960) Smith and Ribbe (1966)
5749	36.6	Carmichael (1965) Smith and Ribbe (1966)
439	44.1	Carmichael (1965) Smith and Ribbe (1966)
5653	47.3	Carmichael (1965) Smith and Ribbe (1966)
1909-261	59.8	Carmichael (1965) Smith and Ribbe (1966)
7002H	83.6	Phillips and Ribbe (1973)
SP-A	95.4	Spencer (1937)

correspond to the F (486.1 nm), D (589.3 nm), and C (656.3 nm) lines of the visible spectrum. The extinction data was analyzed using the program EXCALIBR, developed by Bloss and Reiss (1973). This program employs least-squares regression methods to produce extinction curves from which the exact spindle stage coordinates (S for the rotation axis setting, and M for the microscope stage setting) are calculated for each of the three principle vibration directions at each of the three wavelengths. In addition, the optic axes are located, and the values of the optic axial angle 2V is calculated for each wavelength, usually with estimated errors of less than ~1.0°. The 2V values commonly reported in the literature and in this study are that for sodium (D) light which most nearly approximates the value of 2V for "white" light. Figure 6 is a stereographic projection of the extinction curves for sample #439 used in this study. The principle vibration directions and optic axes are shown, as calculated by EXCALIBR.

Determination of refractive indices

Once the principle vibration directions were located for sodium light, the refractive index for each direction was determined by the double variation method (Bloss, 1961). The Cargille series of immersion oils were used, all of which recently were calibrated to the fifth decimal place over a span of wavelengths using an Abbe refractometer. The Cauchy constants of dispersion were also calculated for each oil.

With each principle vibration direction in turn oriented parallel to the direction of polarization of the microscope's substage polarizer, all three refractive indices can be measured. This is accomplished by

Figure 6

Example of extinction curves (plotted stereographically). The three principle vibration directions and optic axes are shown.

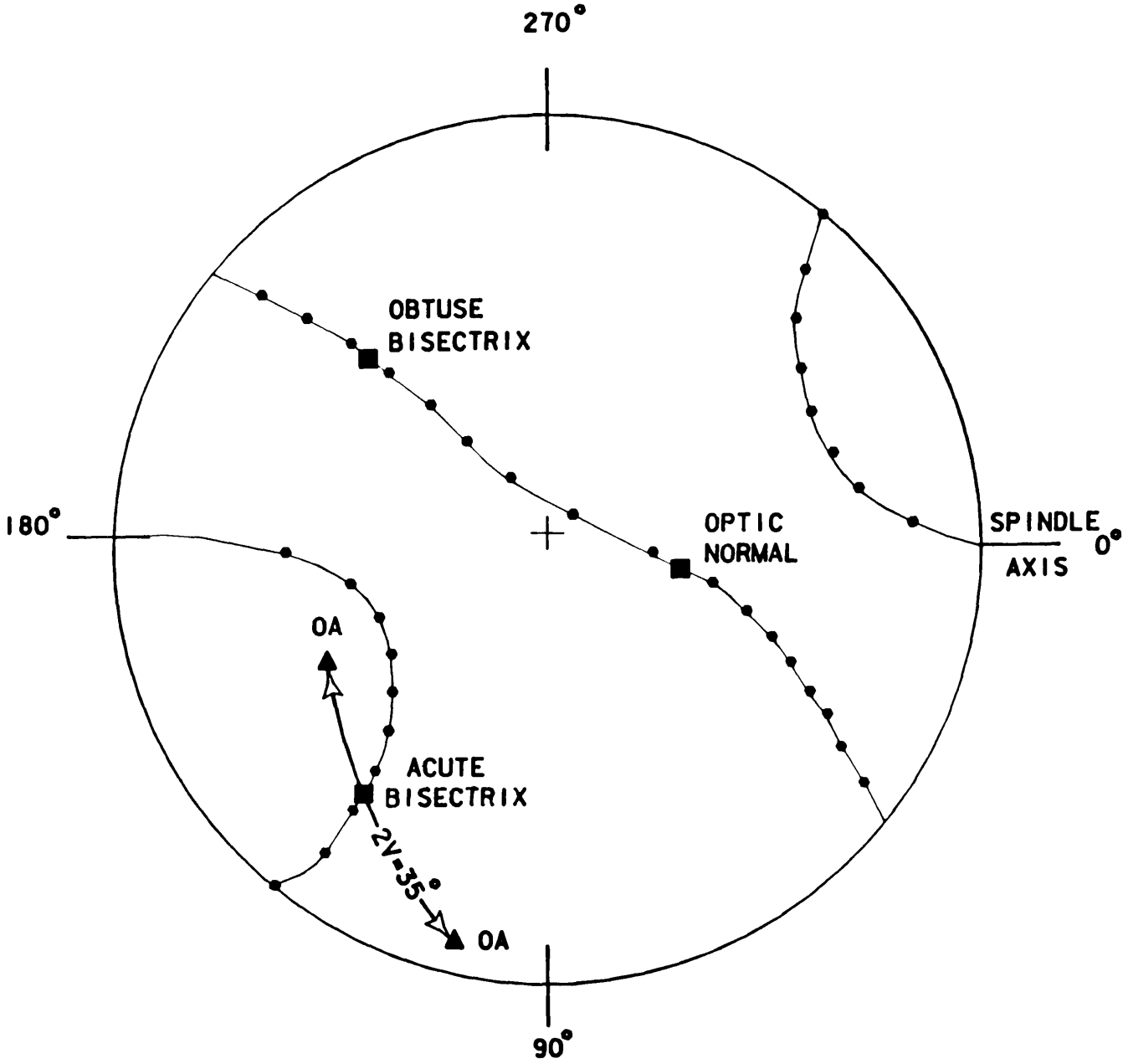
270°
OBTUSE
BISECTRIX
180°
OPTIC
NORMAL
SPINDLE
AXIS
0°
OA
ACUTE
BISECTRIX
2V=35°
OA
90°

immersing the crystal in an oil cell in which the temperature is controlled and can be monitored to ± 0.25°C by use of a thermocouple. The wavelength of incident light is then varied by moving an interference filter attached to the microscope until a match in refractive index occurs between oil and crystal. The Becke line or oblique illumintion method is employed to determine this wavelength. The temperature is then varied so that matches can be determined at successively different wavelengths of light until the whole spectrum has been covered. At the moment that the refractive indices of the oil and crystal match, the temperature is recorded in terms of the millivolt reading of the thermocouple and the wavelength is recorded as the Messort number of the interference filter. These parameters are used as input to a program which converts the millivolt readings to degrees Celcius and the Messort readings to wavelength in nanometers. Other parameters include the refractive index of the oils used, their Cauchy constants, and the amount that the refractive index changes over a 1.0°C change in temperature. The program then calculates by least-squares methods a regression line for refractive index versus wavelength. Figure 7 shows this relationship for the α refractive index of sample #1909-261 with a few of the actual data points plotted (using a Hartmann dispersion graph). Usually three to four oils are needed to span the visible spectrum and approximately 40 to 60 temperature/wavelength combinations are recorded for each of the three refractive indices. With this many data points, the estimated standard errors are usually less than ± 0.0002.

Figure 7

Example of the relationship of refractive index (α in this case) and wavelength. The regression line was calculated by least-squares analysis.

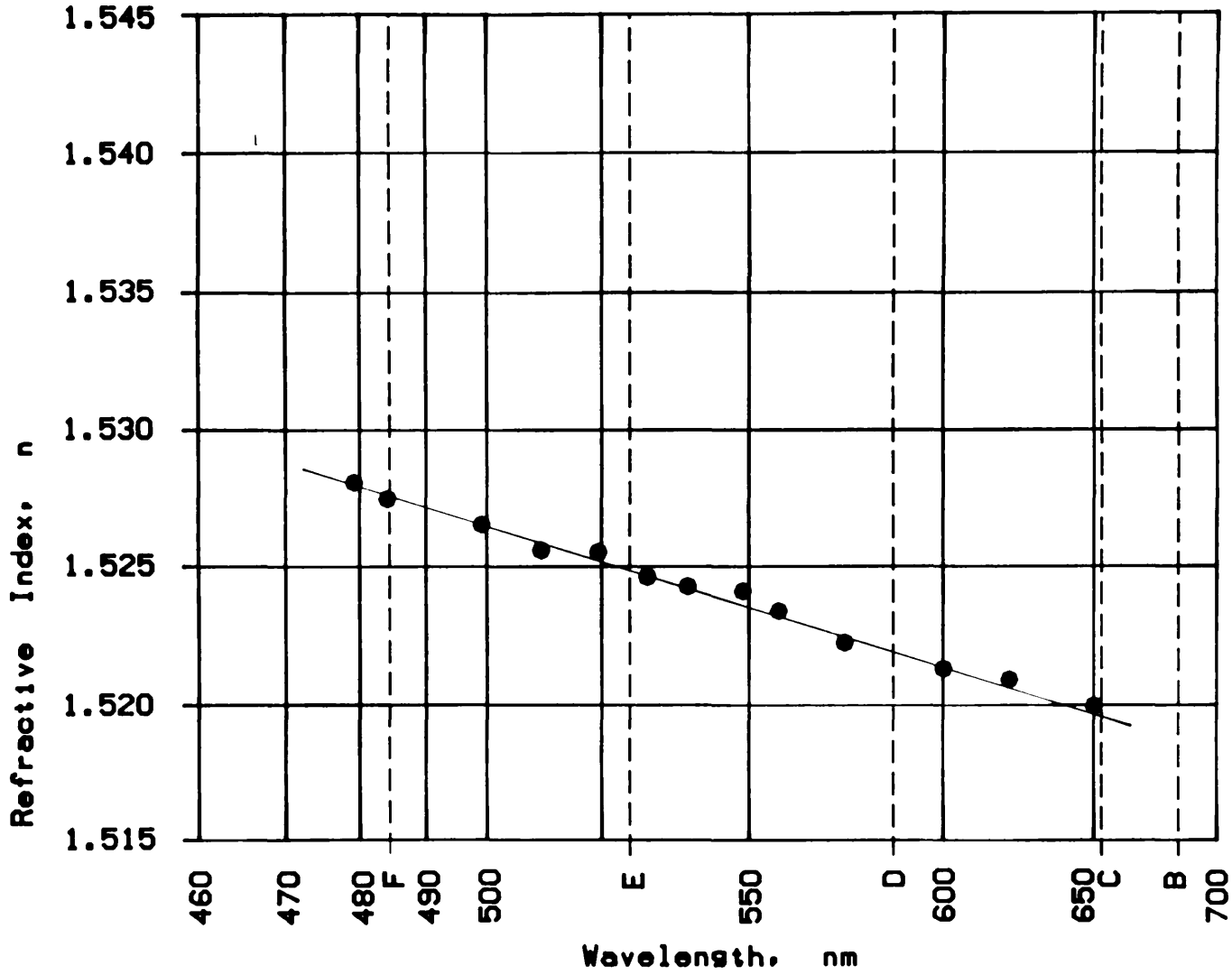
1.545
1.540
1.535
1.530
1.525
1.520
1.515
Refractive Index, n
460
470
480
F
490
500
E
550
D
600
650
C
B
700
Wavelength, nm

Determination of optic orientation

In order to determine the angles between the crystallographic axes a, b, and c and the principle vibration directions for n_a, n_b and n_c, the goniometer head was transferred from the spindle stage to the precession camera, and the crystal was oriented using upper arc (that arc nearer to the crystal) and lower arc adjustments to obtain an a*c* precession photograph. A diagram of an ideal a*c* precession photograph for an alkali feldspar with monoclinic symmetry is shown in Figure 8. Once a correctly oriented photograph of this kind is obtained, it is known that the b axis is located exactly perpendicular to a* and c* and parallel to the x-ray beam; the a axis is exactly parallel to the dial axis of the camera (because it is perpendicular to both a* and c*); and the c axis is exactly perpendicular to both a* and b* (in the plane of the film). Note that b* = b for monoclinic crystals only, and the a*c* photograph is the only one needed to locate all three crystallographic directions. If a crystal were triclinic, b* is only approximately parallel to b and additional photographs would need to be taken.

Using this information, the refractive indices of each principle directon can be designated n_a, n_b or n_c depending on the nearest crystallographic axis to which it is vibrating. The new upper arc and lower arc settings are recorded and all crystallographic axes and principle vibration directions can be located and the angles between them can be calculated. This is achieved by recording the lower and upper arc settings used while collecting optical data (LOARC1 and UPARC1) and the settings which oriented the a*c* precession photograph (LOARC2 and UPARC2). These values are input to EXCALIBR and the

Figure 8

A diagram of an a*c* precession photograph with some of the spots indexed This photograph displays monoclinic symmetry.

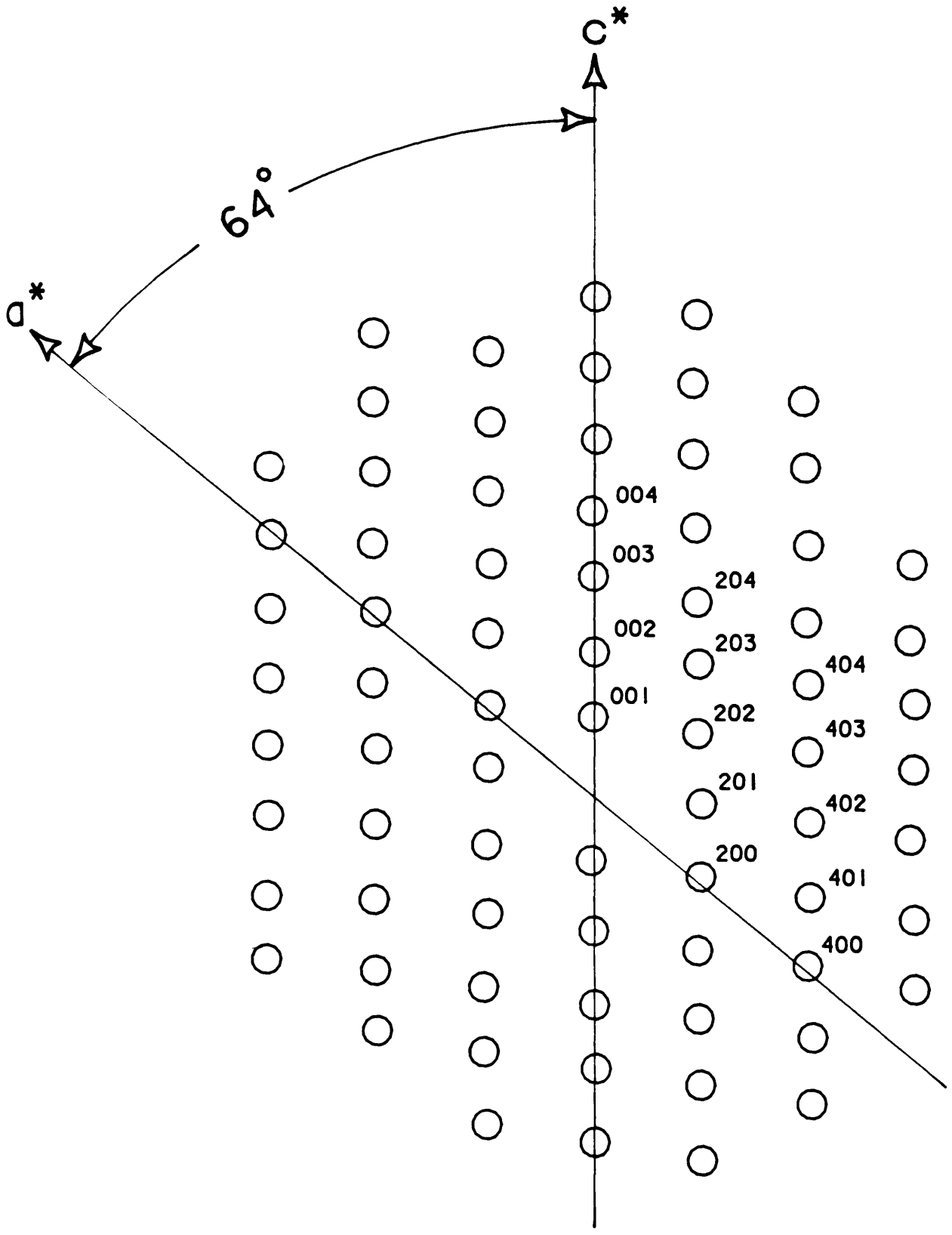
c*
64°
a*
004
003
002
001
204
203
202
201
200
404
403
402
401
400

subroutine ARCRO rotates the principle vibration directions from their original position (at S=0) to the positions they occupy after the crystal is oriented for the a*c* photograph. The angles between these axes can then either be determined graphically using a stereographic projection or by calculating them from the equations which determine the angle between two directions with known S and E coordinates (see Bloss, 1981, p.32).

X-ray Methods

In order to check the orientation of the crystal more precisely for further x-ray work, a 15° double oscillation photograph was taken. It was found that with monoclinic crystals the precession method was sufficient for orienting the crystal and no more adjustments needed to be made. This, however, is not true of triclinic crystals and the oscillation method is needed to further orient these crystals. The oscillation photograph was useful in proving the monoclinicity of the crystals used in this study and in checking for twinning and/or exsolution.

With the a axis located exactly parallel to the dial axis, a back-reflection Weissenberg x-ray photograph can be taken. The back-reflection method is a very precise way to determine the cell dimensions of a single crystal, because this method records only the high angle reflections, i.e., those with 2θ values between 90° and 178°, with a camera diameter of 114.6 mm.

With a direct crystallographic axis (in this case a) located parallel to the dial axis of the camera, two reciprocal axes (in this

case b* and c*) are known to be perpendicular to the dial axis. If the crystal is rotated around the dial axis, 0kl reflections are recorded on the film in the cylindrical cassette. With the back-reflection method, the film is placed such that only the back-reflection spots are recorded. These photographs were exposed to x-rays for 100 to 150 hours because of the small size of the crystals.

It was the back-reflection photograph that revealed that the three samples which were rejected from this study were not "single" crystals. With these crystals, the diffraction spots were diffuse or double. It was noted, however, the a*c* precession photographs of these multiple or composite crystals taken without the layer line screen also showed doubled upper level diffraction spots and could be used to detect more expediently whether or not a particular crystal is suitable for further study.

The individual 0kl spots of the a-axis back-reflection photograph were indexed and the distances between corresponding spots on the upper and lower halves of the film were recorded. This vertical distance is directly related to the 2θ value (1 mm $= 90°2\theta$). The indexing was greatly facilitated by calculating hypothetical distances between corresponding reflections of a high sanidine of composition of 50% orthoclase, 50% albite ($Or_{50}Ab_{50}$). The distances measured from the photographs were usually within one millimeter of these calculated distances. Once a photograph was indexed, photos for other compositions could easily be indexed because the pattern is the same with only minute differences in distances between spots. An ideal diagram of the diffraction spots of a back-reflection photograph obtained from sample #7002H is shown in figure 9.

Figure 9

A diagram of a b*c* back reflection photograph with some of the spots indexed. Measurements taken from this photograph are used in unit cell parameter determination. The large and small circles represent the α_1 and α_2 peaks, respectively, for Cu radiation.

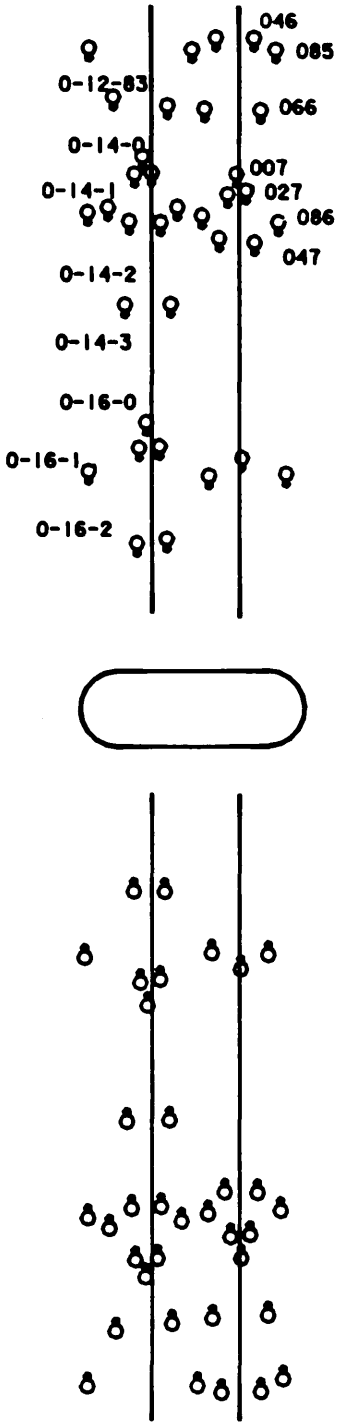
046
085
0-12-83
066
0-14-0
007
0-14-1
027
086
047
0-14-2
0-14-3
0-16-0
0-16-1
0-16-2

The 0kl indices and the 2 measurements were input to a least-squares refinement program modified from Burnham, 1961-62 and 1964-65, and the b and c cell dimensions were calculated. Note that an additional b-axis back-reflection photograph in which h0l reflections are recorded would have increased the accuracy of the cell refinement but the time limitiations of this project did not allow for this second photograph to be taken. Instead, the β angle was measured approximately 10 times and averaged from the a*c* precession photograph. Since the crystals were monoclinic, their α and γ angles are equal to 90.0°. All of these angles were used as input to the program instead of permitting the program to refine on these values.

RESULTS AND DISCUSSION

The values for the refractive indices, n_a, n_b and n_c were plotted against composition in mol % orthoclase for the five samples used in this study. Regression analyses were run on this data using the Statistical Analysis System, SAS, (Helwig and Council, 1979) and it was determined that a linear relationship exists between the refractive indices (R.I.'s) and composition. See Figure 10. As expected, the lines for n_b and n_c cross, and do so at a composition of $\sim Or_{72}$. At this point, 2V passes through 0°; a crystal at this exact compostition and structural state should be optically uniaxial, although in fact still monoclinic in symmetry. Because the refractive indices appear to vary linearly with composition, it should be noted that 2V cannot be linear as previously suggested in the literature; the equation relating refractive indices to 2V is a complex trigonometric function. Using the lines determined from the regression analyses of refractive indices, theoretical 2V values were calculated at increments of 5 mor % Or. This produced a sigmoidal curve for 2Vx just as it did for the K-rich feldspars (cf. Figure 3). Experimental values of 2Vx (plotted in Figure 10) support this trend. There is a significant amount of scatter with regard to experimental 2Vx values which is most likely due to compositional and structural state factors as yet unaccounted for. See Table 2 for a summary of experimental results for the samples used in this study. Figure 11 shows stereographic projections of the optic orientations of the three samples for which all optic and x-ray properties were determined on the same grain. Note that between the

Figure 10

Linear relationship between refractive index and composition for the analbite-high sanidine series. The n_b and n_c lines cross at ~Or_{72}. The 2Vx curve, calculated from the regression lines, is sigmoidal. The small symbols represent the three composite crystals which were not used in the regression analysis. Note, however, that they do not deviate appreciably from the lines.

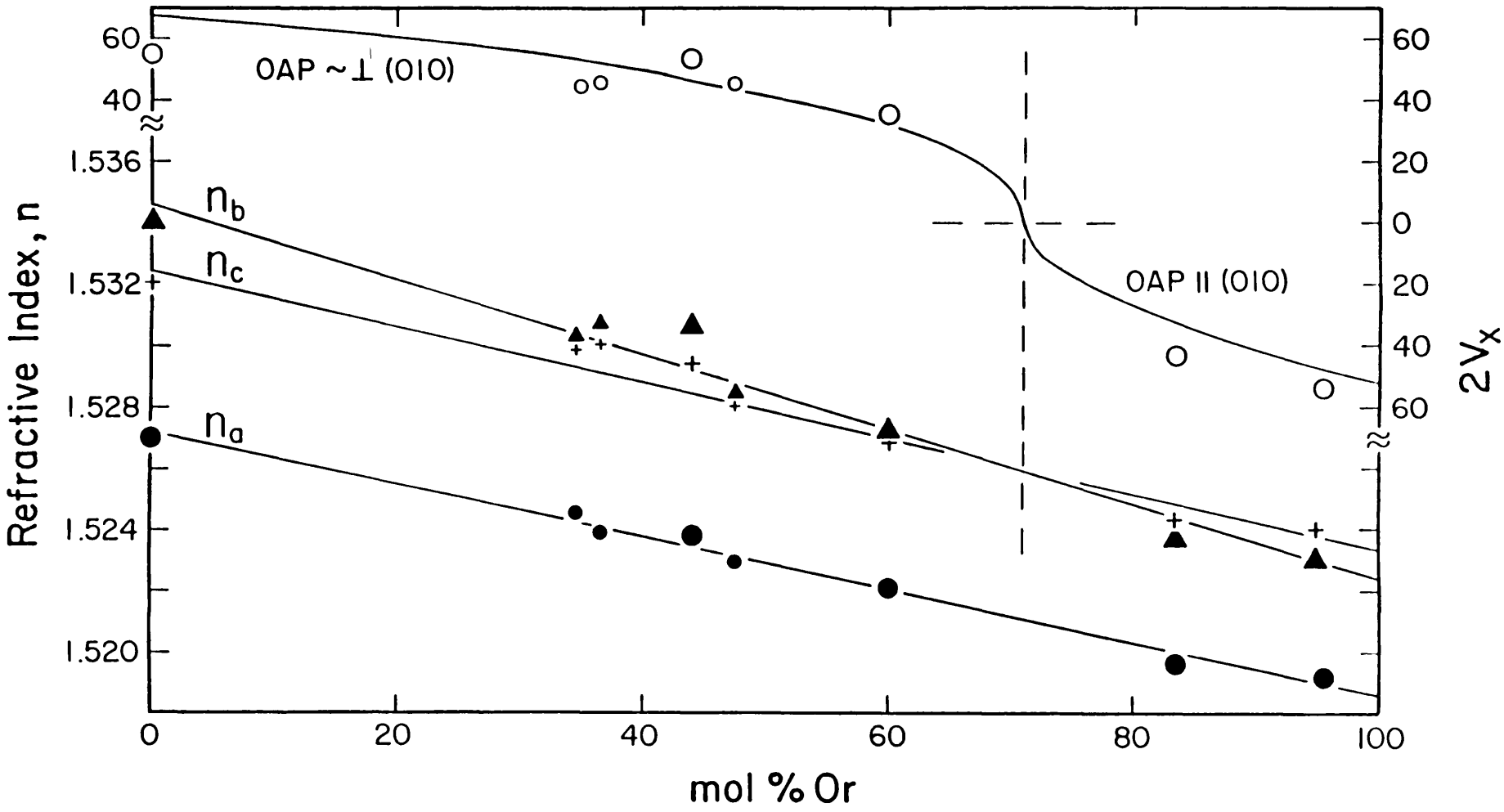
60
40
1.536
1.532
1.528
1.524
1.520
Refractive Index, n
OAP ~⊥ (010)
OAP II (010)
n_b
n_c
n_a
0
20
40
60
80
100
mol % Or
60
40
20
0
20
40
60
$2V_x$

Table 2

Summary of experimental results (optical and x-ray) for the samples used in this study. Three of the samples have a complete set of data, all of which were collected from the same grain. (Note: optical data collected in part by Mr. ShuChun Su, Virginia Tech).

SAMPLE	COMPOSITION (mol % Or)	OPTICAL DATA				X-RAY DATA	
		n_a	n_b	n_c	2V	$\underline{a}$ (Å)	$\underline{b}$ (Å)
HIGH ALBITE*	0.0	1.527	1.534	1.532	45-55		
439	44.1	1.5238	1.5306	1.5292	53.3	12.994	7.163
1909-261	59.8	1.5221	1.5271	1.5268	35.3	13.004	7.172
7002H	83.6	1.5196	1.5237	1.5243	42.6	13.033	7.170
SP-A*	95.4	1.5192	1.5230	1.5240	53.8		

Composite crystals (not used in regression analysis):

3112	34.6	1.5245	1.5303	1.5298	44.3		
5749	36.6	1.5239	1.5307	1.5300	44.7		
5653	47.3	1.5229	1.5284	1.5280	45.3		

*Data obtained from the literature

Figure 11

Stereographic projections of the optic orientations for three of the samples. Angles between crystallographic axes and principle vibration directions are labeled.

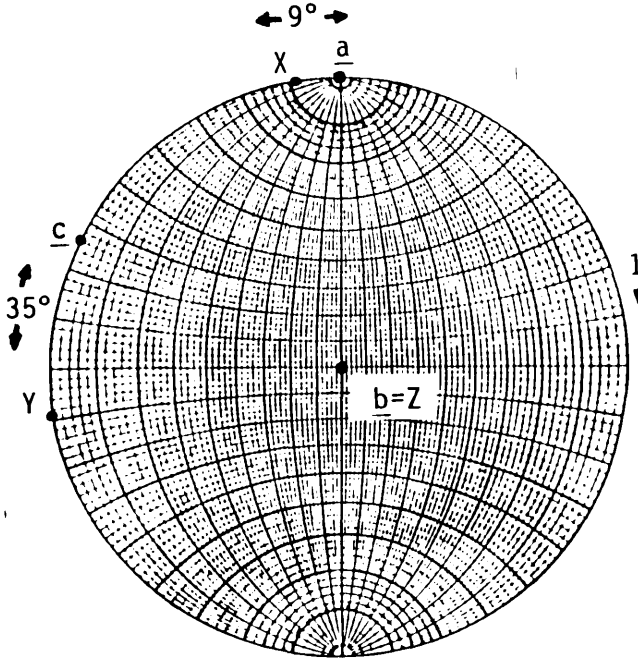

Sample #439

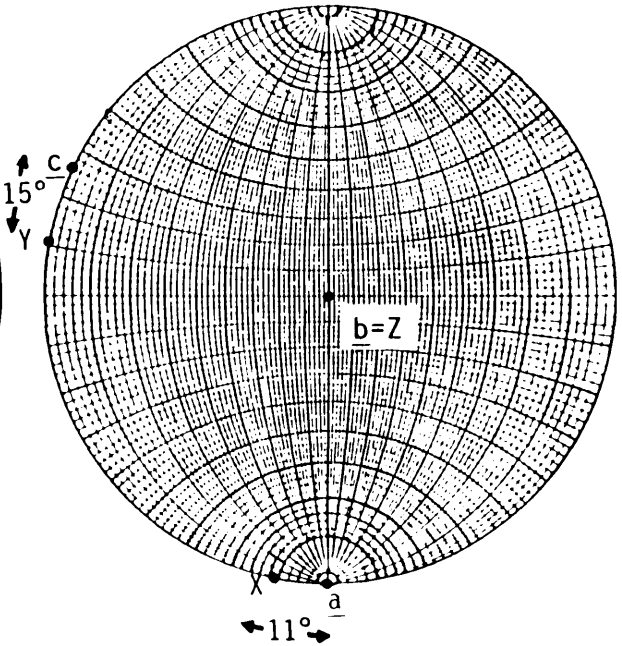

Smaple #1909-261

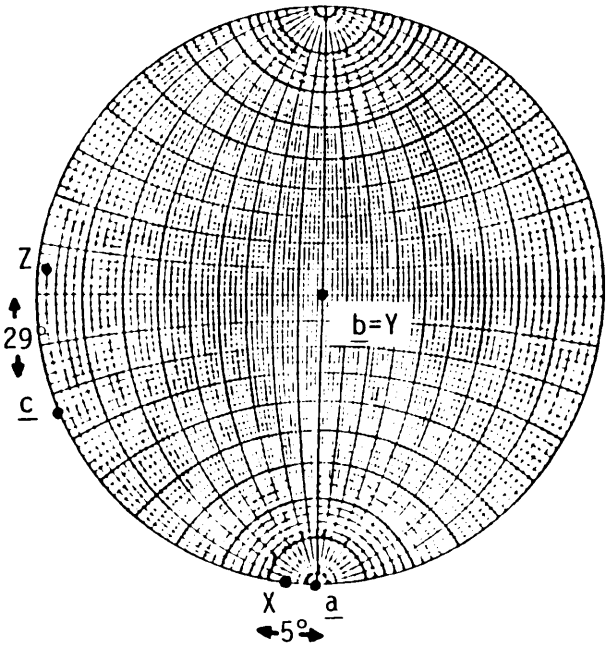

Sample #7002H

samples #1909-261 and #7002H The optic axial plane inverted resulting in a switch in optic orientation i.e., $\underline{b}$ = Z (or γ) in sample #1909-261 while $\underline{b}$ = Y (or β) in sample #7002H.

In an attempt to correct for minor substituents (CaO, SrO, BaO, FeO), the Gladstone-Dale equation (as modified by Bloss et al., 1983) which relates specific refractive index (α , β or γ) to density and wt % oxide:

$$\frac{n - 1}{D} = k_i w_i,$$

where n = α , β or γ ; D = density; k_i = the Gladstone-Dale constant for the oxide i; and w_i = the wt % of the oxide i, was used. It was hoped that k_i values could be determined specifically for alkali feldspars and used to correct the refractive indices of each sample to what they would be for "ideal" compositions of alkali (Na, K) feldspars. Using refractive index and compositional data for a series of heated feldspars (Spencer, 1937; Smith and Ribbe, 1966), regression analyses were employed to determine k values for each oxide. But because the data were so limited in range of composition and structural state, meaningful correlations were not achieved. The need for some sort of correction factor for minor substituents can be empirically seen, for example, in the case of sample #439 (Figure 10). Its refractive indices are furthest from the regression lines, but it also has the highest anorthite content, and anorthite has considerably higher refractive indices than either Na- or K-feldspar.

In order to apply any corrections for composition, the exact compositions for each sample used in this study must be determined

through microprobe analysis. For this study, compositions used were from the analyses of Smith and Ribbe (1966) who collected microprobe data an numerous alkali feldspars, including the ones used here. But there is most probably a chemical variation (though slight) from grain to grain within a particular sample. Once microprobe analysis is complete, a more exact location of the data points with respect to Or content will be achieved.

It also must be noted that variations in structural state will also need to be corrected for. As mentioned earlier, the samples chosen for this study were all assumed to be of "high" structural state but due to the fact that the samples were of natural origin (except the heated albite taken from the literature) there must be some variation due to the differences in formation temperatures and cooling rates. Indeed, when the three samples for which the b and c cell dimensions were determined are located on the b-c plot (see Figure 12) it can be seen that small differences in structural state do occur. Using information obtained from cell parameters of a number of samples, a correction factor must be determined and applied in addition to the correction for compositional differences.

It can be seen that even though the three "composite" crystals are not homogenous, they yield data very close to the curves generated by using only single crystals (see Figure 10). In fact, when they are included in the regression, the lines do not change appreciably. Nor do the 2V values for these crystals deviate from the trend of the sigmoidal curve. Apparently minor amounts of twinning and/or exsolution do not greatly perturb refractive indices, at least for these grains.

Figure 12

Location of three of the samples on the b-c plot. There are slight differences in structural state for these samples.

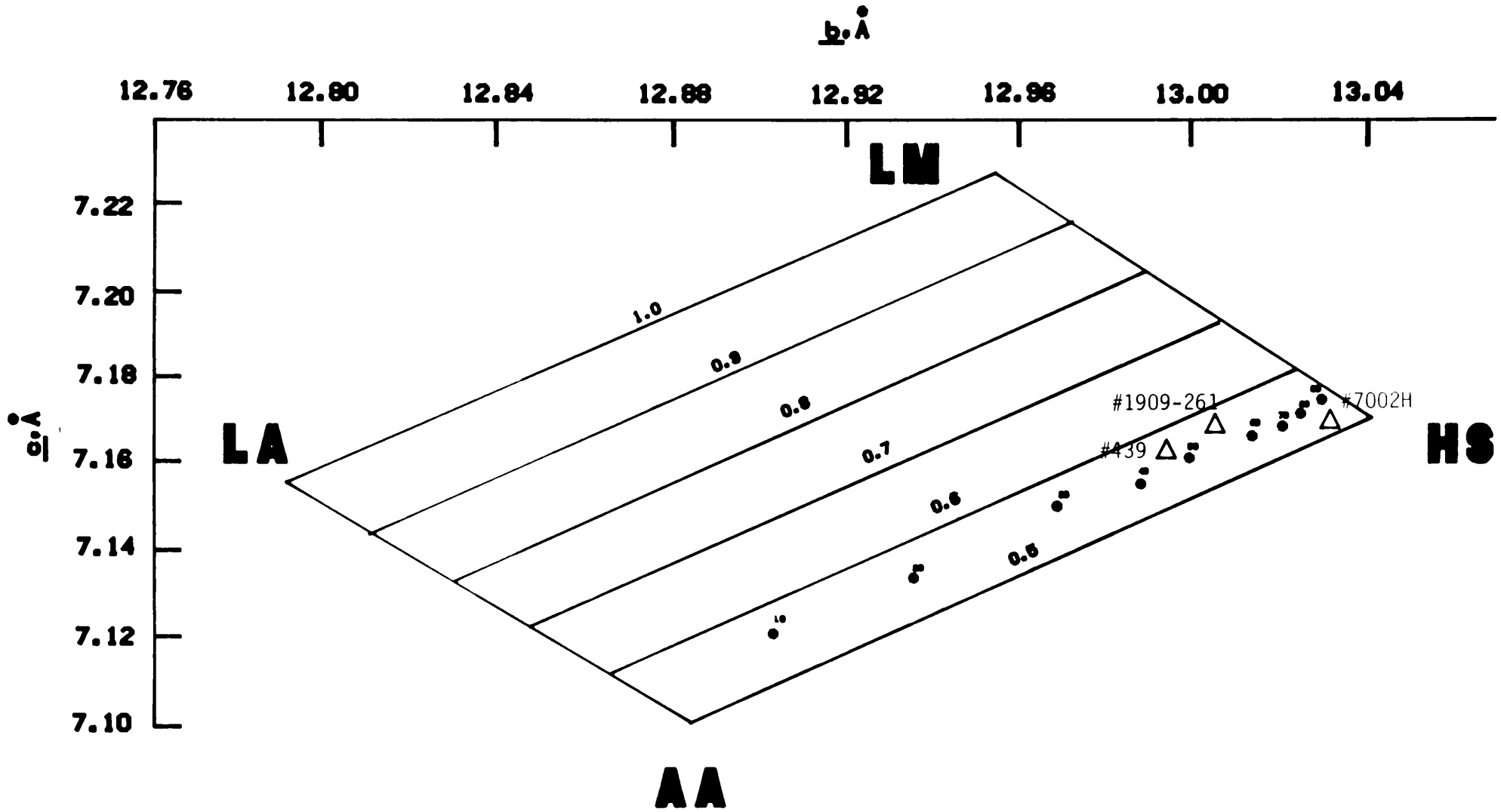
b, Å
12.76
12.80
12.84
12.88
12.92
12.96
13.00
13.04
LM
7.22
7.20
7.18
7.16
7.14
7.12
7.10
c, Å
LA
HS
AA
1.0
0.9
0.8
0.7
0.6
0.5
#1909-261
#7002H
#439

In contrast with the 2V curve which has a significant amount of scatter, the experimental values for n_a do not deviate appreciably from the regression line which has the highest R^2 value -- 0.99. The refractive index, n_a, seems to be less sensitive to minor structural and chemical changes. As such, it may prove to be the best indicator of Or content for natural high temperature alkali feldspars.

CONCLUSIONS

Although more samples need to be added to the data base it has been shown that refractive indices vary linearly with composition for the high temperature alkali feldspars. Of the three refractive indices, the n_a (or α) line has the least amount of scatter (assumed to be produced by slight variations in structural state and minor substituents) and proves to be the most accurate parameter with which to determine composition for high temperature alkali feldspars.

Because refractive indices vary linearly with composition 2V must not be a linear function; in fact it is a sigmoidal function with 2Vx passing through 0° at $\sim Or_{72}$ as the optic axial plane inverts from approximately perpendicular to (010) in Na-rich to parallel to (010) in K-rich feldspars.

A preliminary diagram with 2V contours plotted using this new data for the analbite-high sanidine series along with existing data is shown in Figure 13. Note that composition and structural state are plotted against each other instead of the b and c cell dimensions so that the refractive index lines of each limiting series plot linearly (Su, pers. comm.).

Precise determinative curves cannot be calculated at this stage because grains used in this study lack microprobe analysis which will shift their positions slightly with respect to Or content. In addition, variences in structural state and minor substituents also remains uncorrected for. Once these corrections can be made, this data will contribute to an even better understanding to the relationships between

optical properties, composition, and structural state of not only high temperature but all alkali feldspars.

Figure 13

Plot of structural state vs. composition with 2V contours. Planes of refractive index are also shown. Plot drawn using existing data for the K-rich feldspars (Su, 1984) and new experimental data for the analbite-high sanidine series.

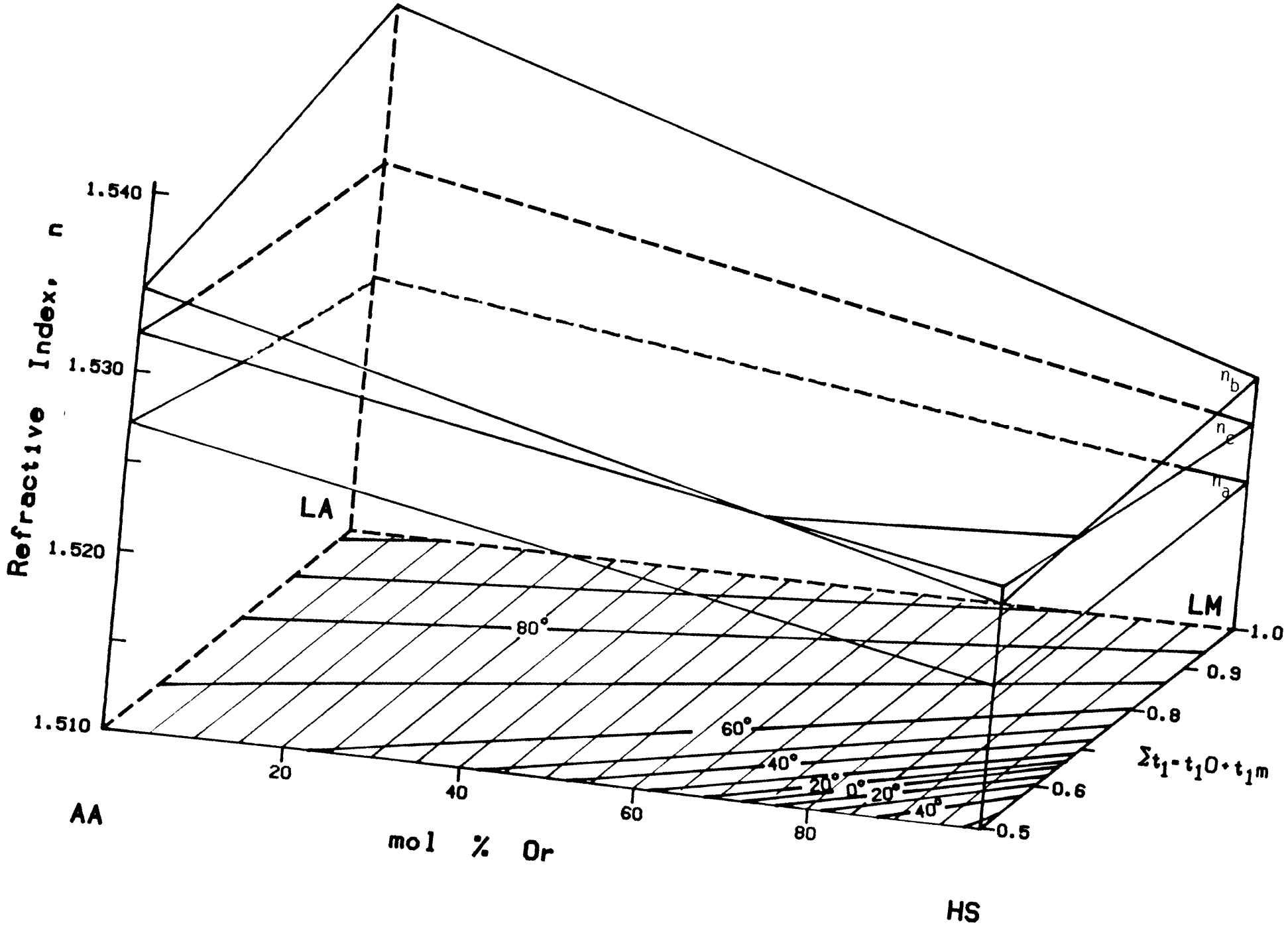
Refractive Index, n
1.540
1.530
1.520
1.510
LA
LM
n_b
n_c
n_a
80°
60°
40°
20°
0°
20°
40°
20
40
60
80
AA
mol % Or
1.0
0.9
0.8
0.6
0.5
$\Sigma t_1 - t_1 0 + t_1 m$
HS

REFERENCES

1.) Bloss, F.D. (1961). An Introduction to the Methods of Optical Crystallography. Holt, Rinehart and Winston: New York, 294 pp.

2.) Bloss, F.D. (1981). The Spindle Stage: Principles and Practice. Cambridge Univ. Press: Cambridge, 340 pp.

3.) Bloss, F.D., Mickey Gunter, ShuChun Su, and H.E. Wolfe (1983). Gladstone-Dale constants: A New Approach. Canadian Mineral. 21, 93-99.

4.) Bloss, F.D., and D. Riess (1973). Computer Determination of 2V and Indicatrix Orientation from Extinction Data. Am. Mineral. 58, 1052-1061.

5.) Burnham, Charles W. (1961-62). Lattice Constant Refinement. Anuual Report of Dir. of the Geophysical Lab., 132-135.

6.) Burnham, Charles W. (1964-65). Refinement of Lattice Parameters Using Systematic Correction Terms. Op. cit., 200-202.

7.) Carmichael, I.S.E. (1960). The Feldspar Phenocrysts of some Tertiary Glasses. Min. Mag., 32, 587-608.

8.) Carmichael, I.S.E. (1965). Trachytes and their Feldspar Phenocrysts. Min. Mag., 34, 107-125.

9.) Hauser, J. and H.-R. Wenk (1976). Optical Properties of Composite Crystals (Submicroscopic Domains, Exsolution Lamellae, Solid Solutions). Z. Kristallogr. 143, 188-219.

10.) Helwig, J.T. and K.A. Council, eds. (1979). SAS User's Guide. SAS Institute Inc., Cary, North Carolina.

11.) Hewlett, C.G. (1959). Optical Properties of Potassic Feldspars. Geol. Soc. Am. Bull. 70, 511-538.

12.) Phillips, M.W. and P.H. Ribbe (1973). The Structures of Monoclinic Potassium-Rich Feldspars. Am. Mineral., 58, 263-270.

13.) Kroll, H. and P.H. Ribbe (1983). Lattice Parameters, Composition and Al,Si Order in Alkali Feldspars. In P.H. Ribbe, Ed., Feldspar Mineralogy, Second Ed., Reviews in Mineralogy, 2, 57-99. Mineral. Soc. Am., Washington, D.C.

14.) Smith, J.V. and P.H Ribbe (1966). X-ray-emission Microanalysis of Rock-forming Minerals. III. Alkali Feldspars. J. Geol. 76, 197-216.

15.) Spencer, E. (1937). The Potash-soda Feldspars I. Thermal Stability. Mineral. Mag. 24, 453-494.

16.) Stewert, D.B. and P.H. Ribbe (1969). Structural Explanation for Variations in Cell Parameters of Alkali Feldspar with Al/Si Ordering. Am. J. Sci. 267-A, 144-462.

17.) Stewert, D.B. and P.H. Ribbe (1983). Optical Properties of Feldspars. In P.H. Ribbe Ed., Feldspar Mineralogy, Second Ed., Reviews in Mineralogy, 2, 121-139. Mineral. Soc. Am., Washington D.C.

18.) Su, S.C., F.D. Bloss, and P.H. Ribbe (1984). Optic Axial Angle, a Precise Measure of Al,Si Ordering in T_1 Tetrahedral Sites of K-rich Alkali Feldspars. Am. Mineral. 69, 440-448.

19.) Tuttle, O.F., and N.L. Bowen (1950). High Temperature Albite and Contiguous Feldspars. J. Geol. 58, 572-583.